Cis and trans interactions between atlastin molecules during membrane fusion

Tina Y. Liu[a], Xin Bian[b,1], Fabian B. Romano[a], Tom Shemesh[c], Tom A. Rapoport[a,2], and Junjie Hu[b,d]

[a]Howard Hughes Medical Institute and Department of Cell Biology, Harvard Medical School, Boston, MA 02115; [b]Tianjin Key Laboratory of Protein Sciences, Department of Genetics and Cell Biology, College of Life Sciences, Nankai University, Tianjin 300071, China; [c]Faculty of Biology, Technion–Israel Institute of Technology, Haifa 32000, Israel; and [d]National Laboratory of Macromolecules, Institute of Biophysics, Chinese Academy of Science, Beijing 100101, China

Contributed by Tom A. Rapoport, March 6, 2015 (sent for review February 18, 2015; reviewed by Reinhard Jahn and William T. Wickner)

Atlastin (ATL), a membrane-anchored GTPase that mediates homotypic fusion of endoplasmic reticulum (ER) membranes, is required for formation of the tubular network of the peripheral ER. How exactly ATL mediates membrane fusion is only poorly understood. Here we show that fusion is preceded by the transient tethering of ATL-containing vesicles caused by the dimerization of ATL molecules in opposing membranes. Tethering requires GTP hydrolysis, not just GTP binding, because the two ATL molecules are pulled together most strongly in the transition state of GTP hydrolysis. Most tethering events are futile, so that multiple rounds of GTP hydrolysis are required for successful fusion. Supported lipid bilayer experiments show that ATL molecules sitting on the same (cis) membrane can also undergo nucleotide-dependent dimerization. These results suggest that GTP hydrolysis is required to dissociate cis dimers, generating a pool of ATL monomers that can dimerize with molecules on a different (trans) membrane. In addition, tethering and fusion require the cooperation of multiple ATL molecules in each membrane. We propose a comprehensive model for ATL-mediated fusion that takes into account futile tethering and competition between cis and trans interactions.

endoplasmic reticulum | GTPase | lipid bilayer | membrane docking | spastic paraplegia type 3A gene

The endoplasmic reticulum (ER) consists of tubules and sheets connected into a characteristic network by membrane fusion (1–3). In contrast to heterotypic fusion between viral and cellular membranes or between intracellular transport vesicles and target membranes, the fusing ER membranes are identical (i.e., homotypic fusion). The mechanism of heterotypic fusion has been studied extensively, leading to the concept that a conformational change of a viral fusion protein or the assembly of SNARE proteins pulls two opposing membranes together so that they can fuse (4–7). Recently, some insight has been obtained into homotypic ER fusion as well. This process is mediated by the atlastins (ATLs) in metazoans and by Sey1p/ROOT HAIR DEFECTIVE3 (RHD3)-related proteins in yeast and plants (8, 9).

The ATLs and Sey1p/RHD3 are membrane-bound GTPases that belong to the dynamin family (reviewed in refs. 10, 11). They contain cytosolic N-terminal GTPase (G) and helical bundle domains, followed by two closely spaced transmembrane (TM) segments and a cytosolic C-terminal tail (12–14). A role for the GTPases in ER fusion is suggested by the observation that their depletion or mutational inactivation leads to long, nonbranched tubules or fragmented ER (8, 9). Nonbranched ER tubules are also observed on expression of dominant-negative ATL mutants (8, 12). In addition, the fusion of ER vesicles in *Xenopus laevis* egg extracts is prevented by ATL antibodies or a cytosolic fragment of ATL (8, 15), and the fusion of the ER in mating yeast cells is delayed on *SEY1* deletion (16). Most convincingly, proteoliposomes containing purified ATL, Sey1p, or RHD3 undergo GTP-dependent fusion in vitro (9, 13, 16, 17). Defects in ATL-mediated ER fusion can cause hereditary spastic paraplegia, a neurodegenerative disease characterized by the shortening of the axons in corticospinal motor neurons, leading to progressive spasticity and weakness of the lower limbs (13, 18).

How exactly the ATLs and Sey1p/RHD3 fuse membranes is not well understood. Crystal structures of ATL and biochemical experiments have not resulted in a coherent model. Initial structures of the N-terminal cytosolic domain of human atlastin-1 (ATL1) revealed two different conformations (13, 14). In both conformations, a dimer is formed between the two G domains, but in one conformation (crystal form 2; *SI Appendix*, Fig. S1), the subsequent three-helix bundle (3HB) domains point in opposite directions, whereas in the other (crystal form 1; *SI Appendix*, Fig. S1), they are parallel to one another. These structures were interpreted as "prefusion" and "postfusion" states, in which the two ATL molecules would either tether two opposing membranes or sit in the same membrane after fusion (13).

Because the prefusion structure was crystallized in the presence of GDP and inorganic phosphate (P_i) and the postfusion structure was crystallized in the presence of GDP, it was proposed that GTP hydrolysis would induce this conformational change, resulting in the apposed membranes being pulled together for fusion (13). Both structures contained only bound GDP, however, raising doubts that the conformational change is induced by GTP hydrolysis. In addition, biochemical experiments suggested that ATL dimers form in the GTP-bound state and dissociate into monomers in GDP, given that dimerization was much more pronounced in the presence of nonhydrolyzable

Significance

The membrane-anchored GTPase atlastin (ATL) mediates the fusion of endoplasmic reticulum membranes into a network of tubules and sheets, but the mechanism of ATL function is still poorly understood. Here we show that vesicle fusion is preceded by GTP hydrolysis-dependent tethering, caused by the interaction of ATL molecules in opposing membranes. GTP hydrolysis also dissociates ATL dimers sitting in the same membrane (cis dimers), generating a pool of ATL monomers that can dimerize with molecules on a different (trans) membrane. Multiple rounds of GTP hydrolysis and the cooperation of several ATL molecules in each membrane are required for a successful fusion event. These results lead to a model of ATL-mediated fusion that also may have implications for SNARE-mediated fusion.

Author contributions: T.Y.L., X.B., F.B.R., T.S., T.A.R., and J.H. designed research; T.Y.L., X.B., F.B.R., T.S., and J.H. performed research; T.Y.L., X.B., F.B.R., T.S., T.A.R., and J.H. analyzed data; and T.Y.L. and T.A.R. wrote the paper.

Reviewers: R.J., Max Planck Institute for Biophysical Chemistry; and W.T.W., Geisel School of Medicine at Dartmouth College.

The authors declare no conflict of interest.

Freely available online through the PNAS open access option.

[1]Present address: Boyer Center for Molecular Medicine, Yale University, New Haven, CT 06519.

[2]To whom correspondence should be addressed. Email: tom_rapoport@hms.harvard.edu.

This article contains supporting information online at www.pnas.org/lookup/suppl/doi:10.1073/pnas.1504368112/-/DCSupplemental.

GTP analogs compared with GDP (13, 14); the high protein concentration during crystallization may have allowed dimerization in GDP.

A third crystal structure (crystal form 3; *SI Appendix*, Fig. S1) led to further confusion. It was obtained in the presence of GMPPNP or GDP plus AlF_4^- (GDP/AlF_4^-) and represents a state before P_i release (19). This structure resembles the post-fusion state rather than the expected prefusion state; the two 3HBs are again parallel, and in fact are even closer to one another. Finally, a structure of GDP-bound *Drosophila* ATL showed a prefusion-like conformation (20).

The different structural and biochemical results have given rise to conflicting models for ATL-mediated membrane fusion. It has been proposed that GTP hydrolysis occurs after fusion, although this is difficult to reconcile with in vitro experiments showing that GTP hydrolysis is required for membrane fusion (21). Other models postulate that GTP binding is sufficient for the tethering of the two membranes through dimerization of ATL molecules sitting in opposing membranes (trans dimer) (9, 13, 22), or that GTP binding and hydrolysis occur in a monomer before trans dimerization (19). It also has been proposed that ATL molecules would interact only in cis, i.e., in the same membrane, rather than tethering opposing membranes before their fusion; the ATL molecules would induce high membrane curvature in both lipid bilayers, which would facilitate their fusion (23).

Here we propose a model that provides a coherent picture of ATL function. We show that GTP hydrolysis is required for membrane tethering, although dimer formation per se can occur with nonhydrolyzable GTP analogs. GTP hydrolysis, and not just GTP binding, is required, because two ATL molecules are pulled together most strongly in the transition state during GTP hydrolysis, and because dimers forming on the same (cis) membrane need to be dissociated to allow ATL molecules to dimerize with molecules on a different (trans) membrane. Tethering and fusion require the cooperation of multiple ATL molecules in each membrane, and multiple cycles of GTP hydrolysis occur before a successful fusion event. These results have implications for ER fusion in vivo.

Results

GTP Hydrolysis Is Required for ATL-Mediated Vesicle Tethering. To study the role of GTP binding and hydrolysis in vesicle tethering and fusion, we first used dynamic light scattering to measure the size increase of proteoliposomes containing purified *Drosophila* ATL (9). In the presence of GTP and Mg^{2+}, when membrane fusion occurs, the mean radius of the vesicles increased by a factor of ~1.5 (Fig. 1*A*). Interestingly, addition of EDTA, which chelates Mg^{2+} and inactivates ATL, partially reversed the size increase. The EDTA-insensitive size increase, which originates from actual fusion of the vesicles, is relatively small; the majority of vesicles are just tethered to one another by ATL molecules. Tethering requires continuous GTP hydrolysis, since no increase in vesicle size was observed with the nonhydrolyzable GTP analog GTPγS, with GDP, or in the absence of nucleotide (Fig. 1*A*). Furthermore, inactivation of ATL's GTPase activity by the addition of GTPγS to a reaction containing GTP also reduced the mean vesicle radius (*SI Appendix*, Fig. S2*A*).

Similar results were obtained by measuring light absorbance at a wavelength of 405 nm in a spectrophotometric plate reader. This assay also monitors vesicle tethering and fusion, because the resulting size increase of the vesicles causes the solution to become turbid. Again, in the presence of GTP, the ATL-containing proteoliposomes increased in size over time, and this size increase was partially reversed by the addition of EDTA (Fig. 1*B*). No size change was seen in the presence of GTPγS or GDP, or in the absence of nucleotide or Mg^{2+} (Fig. 1*B*). Addition of the nonhydrolyzable GTP analog GMPPNP or of GDP/AlF_4^-, which mimics the transition state during GTP hydrolysis, also resulted in no (Fig. 1*B*) or only very little (*SI Appendix*, Fig. S2*B*) vesicle tethering. It should be noted that the latter conditions were used to obtain crystal form 3, i.e., the state in which ATL molecules are most tightly associated with one another (19).

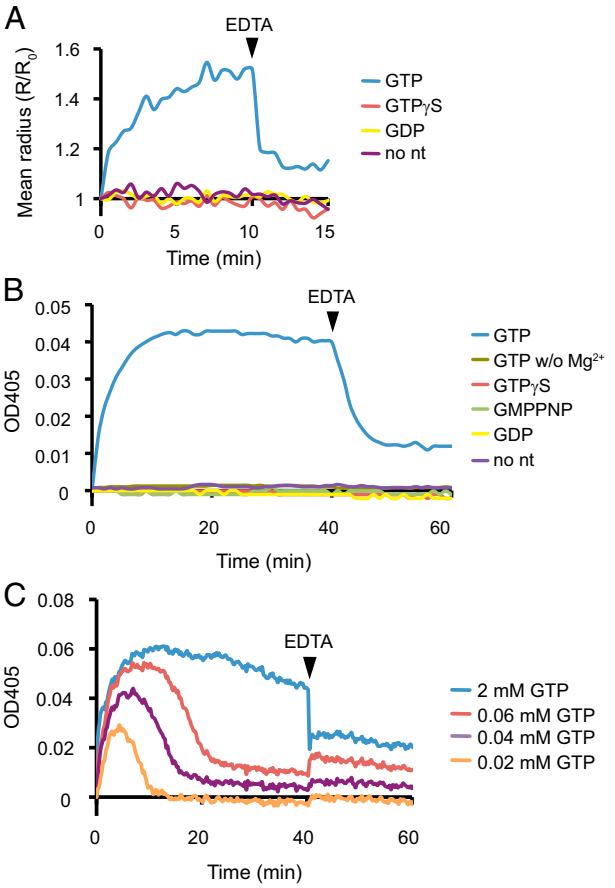

Fig. 1. ATL-mediated vesicle tethering requires continuous GTP hydrolysis. (*A*) No nucleotide (no nt) or the indicated nucleotides were added to ATL-containing proteoliposomes (protein:lipid ratio 1:2,000), and the increase of the apparent hydrodynamic radius of the vesicles was determined by dynamic light scattering. The measurements were normalized to the radius determined at time 0 (R/R_0). EDTA was added after 10 min to chelate Mg^{2+} and inactivate ATL. (*B*) As in *A*, but the increase in vesicle size was measured by the light absorbance at a wavelength of 405 nm. Where indicated, Mg^{2+} was omitted (GTP w/o Mg^{2+}). (*C*) As in *B*, but with ATL reconstituted into vesicles at a 1:1,000 protein:lipid ratio, and with different GTP concentrations added at time 0. The baseline obtained in the absence of GTP was subtracted from each of the curves.

To visualize the tethering and fusion reactions, we reconstituted ATL into vesicles containing phospholipids with either a fluorescent Texas Red or Oregon Green dye attached to their head groups. Samples of the reactions were diluted and spotted onto a glass coverslip, and vesicles stuck to the surface were visualized with a confocal microscope. Before the addition of GTP, the vesicles appeared as red or green punctae (Fig. 2*A*, *Left*); at 5 min after the addition of GTP, large yellow punctae appeared in which the two dyes colocalized, indicating that the differently colored vesicles were associated or fused with one another (Fig. 2*A*, *Middle*). When EDTA was added, most of these large punctae disappeared or became smaller, indicating that many vesicles were untethered (Fig. 2*A*, *Right*). No tethering or fusion was seen in the presence of GDP (Fig. 2*B*), in the absence of nucleotide (Fig. 2*C*), or in the presence of GTPγS (*SI Appendix*, Fig. S3*A*) or GMPPNP (*SI Appendix*, Fig. S3*B*). In the presence of GDP/AlF_4^-, a very low level of tethering was observed, which was not strongly affected by the addition of EDTA (*SI Appendix*, Fig. S3*C*).

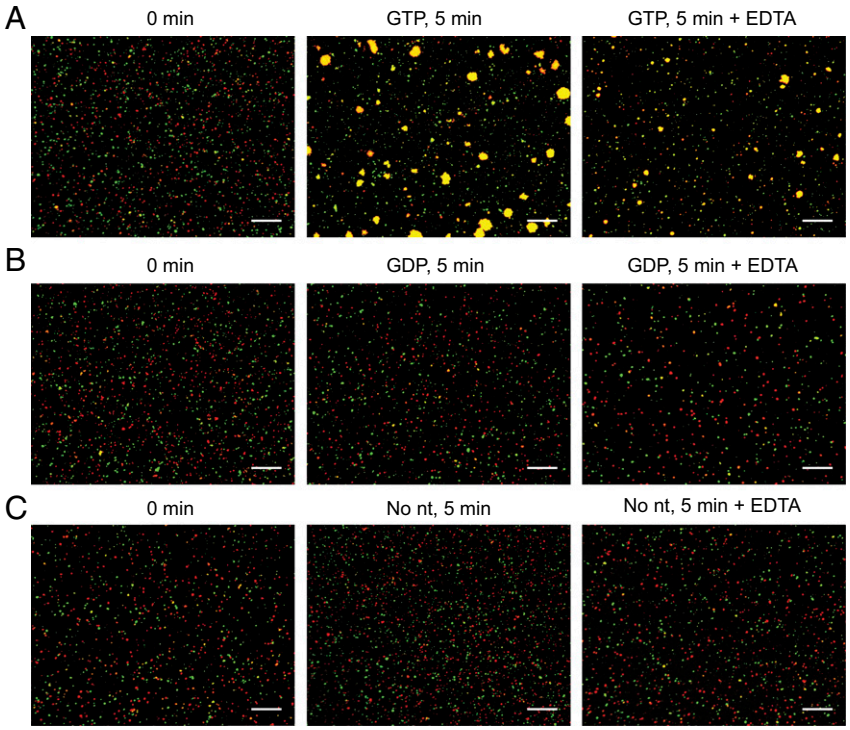

Fig. 2. GTP-dependent tethering and fusion followed by a visual assay. (*A*) ATL-containing proteoliposomes (protein: lipid ratio 1:1,000), which also contained either Texas Red- or Oregon Green-labeled lipids, were mixed at a 1:1 ratio (total lipid concentration: 0.6 mM). One aliquot was analyzed immediately, a second was taken after incubation at 37 °C with 1 mM GTP for 5 min, and a third was obtained after incubation with GTP followed by addition of 10 mM EDTA. All samples were diluted, spotted onto a coverslip, and visualized by confocal microscopy. (Scale bar: 10 μm.) (*B*) As in *A*, but with 1 mM GDP. (*C*) As in *A*, but without nucleotide (nt).

To further demonstrate that tethering requires ongoing GTP hydrolysis, we followed changes in vesicle size by measuring 405-nm absorbance in the presence of different GTP concentrations (Fig. 1*C*). At the lowest GTP concentration, the absorbance increased, but returned to its original level as GTP was consumed. Thus, under these conditions, vesicles transiently tether but do not fuse efficiently. At higher GTP concentrations, tethering became more pronounced and persistent. The absorbance values after the addition of EDTA also increased with the GTP concentration, indicating that fusion became more efficient. Our results show that multiple cycles of GTP hydrolysis occur before a successful fusion event. In addition, they suggest that ATL molecules sitting in different membranes interact with one another only during GTP hydrolysis, a surprising observation given that stable dimerization of the cytosolic domain of ATL can occur with nonhydrolyzable GTP analogs (13, 14).

The Cytosolic Domain of ATL Mediates Membrane Tethering. We next tested whether membrane tethering can be separated from membrane fusion. Specifically, we reasoned that the cytosolic domain of ATL (cytATL) might be sufficient for tethering, but not for fusion. Thus, we generated constructs in which the native TM segments of ATL were replaced with the TM segment of Sec61β (ATL-Sec61β) or with the second TM segment of ATL (cyt-TM2) (Fig. 3*A*). Both mutants were indeed defective in membrane fusion, as measured by a lipid-mixing assay (*SI Appendix*, Fig. S4) (24); however, both were active in membrane tethering, as demonstrated by dynamic light scattering (Fig. 3*B*). As with wild type (WT) ATL, tethering was observed with GTP but not with GTPγS, GMPPNP, GDP, or in the absence of nucleotide. On the addition of EDTA to the GTP-containing reaction, the vesicle size dropped to the original level, consistent with the absence of any fusion. While this manuscript was in preparation, another group also found that tethering requires GTP hydrolysis and can be separated from fusion (25).

Similar results were obtained when the size of the vesicles was followed by absorbance measurements at 405 nm (Fig. 3*C* and *SI Appendix*, Fig. S5). Furthermore, in a visual assay with differently colored proteoliposomes containing ATL-Sec61β, colocalization of the dyes was observed in the presence of GTP, but was almost completely reversed on addition of EDTA (Fig. 4*A*). No tethering was seen in the presence of GDP (Fig. 4*B*), GTPγS (*SI Appendix*, Fig. S6*A*), GMPPNP (*SI Appendix*, Fig. S6*B*), or GDP/AlF_4^- (*SI Appendix*, Fig. S6*C*) or in the absence of nucleotide (Fig. 4*C*).

To further test whether the cytosolic domain of ATL is sufficient for vesicle tethering, we attached a His_8 tag to its C terminus and anchored the construct (cytATL-His) to preformed liposomes containing Ni^{2+}-NTA phospholipids (Fig. 5*A*). As expected, cytATL-His floated with Ni^{2+}-NTA–containing liposomes in a Nycodenz gradient (Fig. 5*B*). No flotation was observed in the presence of imidazole or EDTA, or when the protein was incubated with liposomes lacking Ni^{2+}-NTA lipids. The cytATL-His–containing vesicles showed GTP hydrolysis-dependent tethering in dynamic light scattering (Fig. 5 *C* and *D*) and 405-nm absorbance assays (Fig. 5*E*). As with ATL-Sec61β and cyt-TM2, no tethering was observed with nonhydrolyzable GTP analogs, with GDP, or in the absence of nucleotide. The addition of EDTA or imidazole completely reversed the size increase seen in the presence of GTP (Fig. 5 *C*–*E*). Taken together, these results indicate that the cytosolic domain of ATL is sufficient to promote vesicle tethering, but not fusion.

ATL Molecules Cooperate to Promote Membrane Tethering. Given that each ATL dimer tethers opposing membranes only transiently during GTP hydrolysis, we tested whether the formation of multiple dimers across the two membranes would increase the

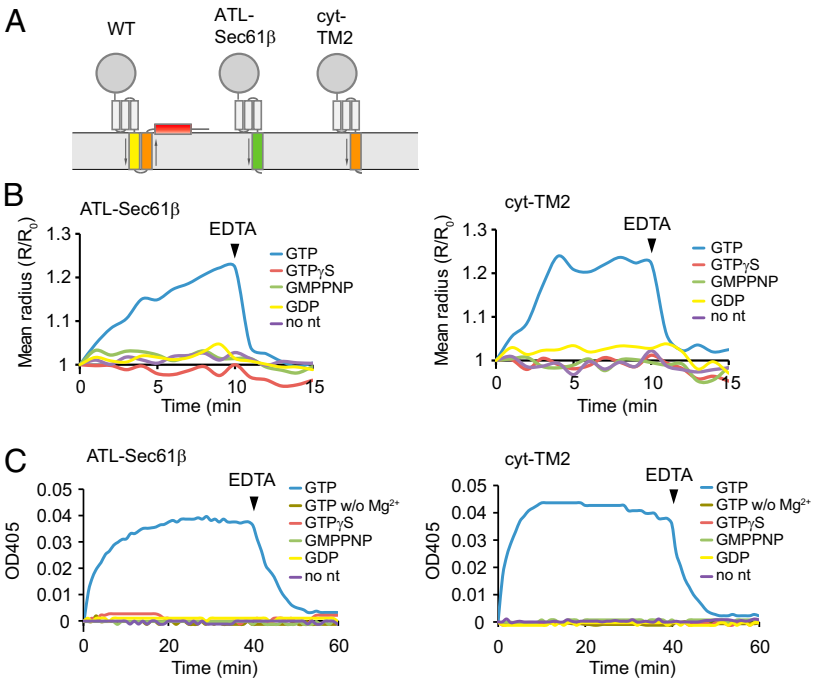

Fig. 3. Membrane tethering mediated by ATL containing different TM segments. (*A*) Schematic of WT ATL and ATL mutants (ATL-Sec61β and cyt-TM2) containing different TM segments. The G domain and the 3HBs are shown in gray, TM1 and TM2 of WT ATL are in yellow and orange, respectively, and the cytosolic C-terminal tail is in red. The TM of ATL-Sec61β is shown in green. The orientation of the TM segments is indicated by arrows. (*B*) The tethering of vesicles containing ATL-Sec61β and cyt-TM2 (protein:lipid ratio 1:2,000) was determined by dynamic light scattering in the presence of different nucleotides (no nt, no nucleotide added). EDTA was added after 10 min to chelate Mg^{2+} and inactivate ATL's GTPase activity. (*C*) As in *B*, but tethering was followed by absorbance at 405 nm, and EDTA was added after 40 min. Where indicated, Mg^{2+} was omitted (GTP w/o Mg^{2+}).

efficiency of tethering. To this end, we distributed the same number of ATL-Sec61β molecules over different numbers of ∼160-nm-diameter proteoliposomes (protein:lipid ratios of 1:5,000 and 1:2,000). These ratios correspond to ∼40 and ∼100 protein molecules per vesicle, respectively. SDS/PAGE analysis confirmed that the samples with different protein:lipid ratios contained the same total amounts of ATL-Sec61β (*SI Appendix*, Fig. S7). The sample with a higher density of ATL-Sec61β per vesicle showed significantly stronger membrane tethering, as determined by dynamic light scattering (Fig. 6*A*). With WT ATL, tethering was also more efficient, with a higher protein density per vesicle (Fig. 6*B*). These results indicate that tethering is more efficient if multiple ATL molecules in the two interacting membranes participate in dimer formation. Increased tethering by WT ATL led to more fusion (Fig. 6*C*). In fact, at the lower protein density, fusion was so inefficient that it could not be detected by light scattering (Fig. 6*B*) and was detected only with the more sensitive lipid-mixing assay (Fig. 6*C*). Thus, multiple ATL molecules on each membrane cooperate to mediate tethering and fusion of vesicles.

Interactions Between the 3HBs of ATL Molecules. We next analyzed the molecular mechanism of ATL in more detail by correlating the structural data with nucleotide-dependent conformational changes of ATL in solution. Specifically, we tested when the 3HB domains of ATL molecules come close to one another during the GTPase cycle. Fluorescent probes incorporated at position 332 of the 3HB of *Drosophila* cytATL should allow fluorescence resonance energy transfer (FRET) when the ATL molecules interact as in crystal form 1 (distance, ∼8 Å) or crystal form 3 (distance, ∼5 Å), but not when interacting as in crystal form 2 (distance, ∼77 Å) (*SI Appendix*, Fig. S1). Although FRET experiments had been performed previously with C-terminal fusions of human cytATL with YFP and CFP (19), the size of the probes and their attachment through a flexible linker raises the possibility that they did not distinguish between dimers of different conformations. Indeed, comparable FRET levels were observed with GMPPNP and GDP/AlF_4^- (19), making it uncertain whether GTP binding or hydrolysis drives a conformational change. We incorporated small fluorescent probes at position 332 of *Drosophila* cytATL by replacing the native Leu codon with an amber codon and suppressing it in *E. coli* with an orthogonal tRNA charged with azidophenylalanine (26); after purification, the proteins were modified with Cy5 or Cy3 fluorescent dyes using Cu^{2+}-free click chemistry. The labeled proteins had GTPase activities comparable to that of WT cytATL (*SI Appendix*, Fig. S8).

On the addition of GTP to a mixture of Cy3- and Cy5- labeled cytATL, the FRET signal increased immediately, and reached a plateau after a short period (Fig. 7 *A* and *B*). A slightly slower increase was seen with GTPγS, but the FRET plateau was about the same. The addition of GDP/AlF_4^- resulted in a much slower increase of FRET, but the final level was significantly higher than in GTP or GTPγS. No increase in FRET was seen upon the addition of GDP or in the absence of nucleotide. These results suggest that GTP binding allows cytATL molecules to rapidly form dimers in which the 3HBs occasionally come close to one another. When cytATL molecules start out in the transition state of GTP hydrolysis (GDP/AlF_4^-), the 3HBs associate much more slowly, but ultimately interact very tightly, likely in the conformation seen in crystal form 3 (*SI Appendix*, Fig. S1).

Consistent with a tight interaction of cytATL molecules in the transition state, the FRET increase due to dimerization in the presence of GDP/AlF_4^- could not be reversed by the addition of unlabeled cytATL (Fig. 7*B*). In contrast, Cy3- and Cy5-labeled cytATL dimers formed in the presence of GTP or GTPγS were dissociated by unlabeled cytATL (Fig. 7*B*). As expected, EDTA also dissociated the dimers formed in GTP and GTPγS (*SI Appendix*, Fig. S9); however, EDTA did not affect the dimers

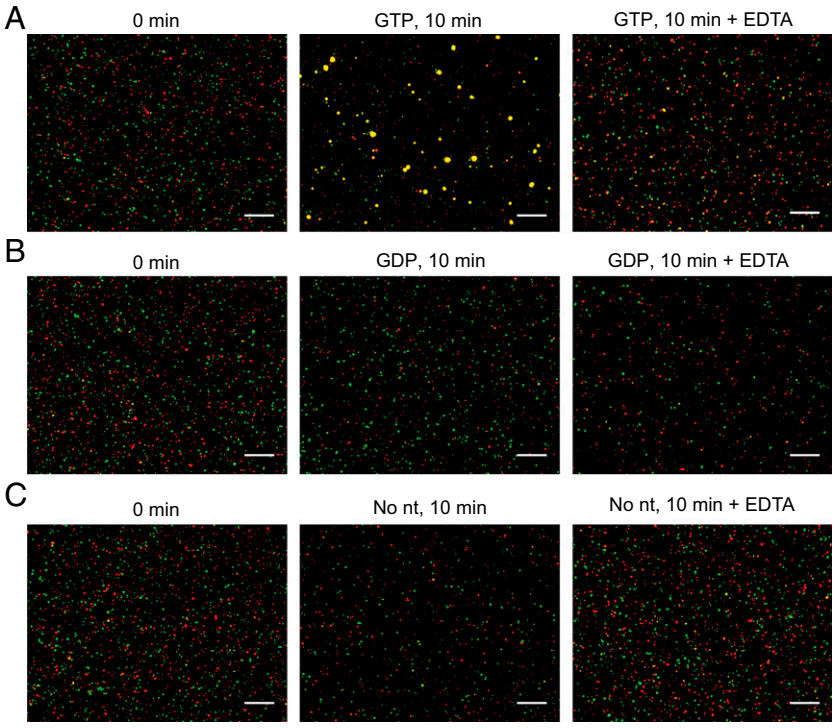

Fig. 4. Membrane tethering by ATL-Sec61β followed with a visual assay. (*A*) Proteoliposomes containing ATL-Sec61β (protein:lipid ratio 1:1,000) and either Texas Red- or Oregon Green-labeled lipids were mixed at a 1:1 ratio (total lipid concentration: 0.6 mM). One aliquot was analyzed immediately, a second was taken after incubation at 37 °C with 1 mM GTP for 10 min, and a third was obtained after incubation with GTP followed by addition of 10 mM EDTA. All samples were diluted, spotted onto a coverslip, and visualized by confocal microscopy. (Scale bar: 10 μm.) (*B*) As in *A*, but with 1 mM GDP. (*C*) As in *A*, but without nucleotide (nt).

generated with GDP/AlF_4^-, probably because the Mg^{2+} ion is occluded in the active site in the transition state conformation. These data confirm that the transition state dimer is more stable than the GTP-bound dimer. The difference between GTP and GTPγS shows that GTP hydrolysis contributes significantly to the dissociation rate of ATL dimers.

To confirm that the interaction of ATL molecules is strongest in the transition state of GTP hydrolysis, we performed flotation experiments. Proteoliposomes containing full-length ATL were incubated with cytATL in the presence of different nucleotides and subjected to flotation in a Nycodenz gradient. The amount of cytATL associated with the vesicles was determined by SDS/PAGE and Coomassie Blue staining. Coflotation of cytATL was more pronounced with GDP/AlF_4^- compared to that with GTPγS, GDP, or no nucleotide (Fig. 7*C*).

Taken together, these results indicate that ATL molecules associate rapidly on GTP binding and form a very stable dimer in the transition state during hydrolysis of the γ-phosphate bond. The dimers dissociate back into monomers either in the GDP-bound state after P_i release or in the nucleotide-free state.

Cis and Trans Interactions of ATL Molecules. We next tested by FRET whether ATL molecules can interact in cis, i.e., when they are located in the same membrane. To do so, we generated a supported planar bilayer with liposomes containing Ni^{2+}-NTA phospholipids, then added a mixture of C-terminal His_8-tagged cytATL proteins with Cy3 or Cy5 probes in the 3HB at position 332. At the chosen concentration, both labeled proteins bound stably to the supported bilayer; no decrease in fluorescence was observed when the bilayer was washed with buffer. Because the labeled cytATL-His molecules are bound to a planar membrane, they can interact only in cis; the absence of molecules in bulk solution precludes any trans interactions. Before the addition of nucleotide, no FRET was observed (Fig. 8*A*); however, significant FRET was seen after addition of different nucleotides. FRET was confirmed by the finding that bleaching of the acceptor dye resulted in a significant increase in fluorescence of the donor dye (shown for a reaction with GDP/AlF_4^- in *SI Appendix*, Fig. S10*A*).

The FRET signal was strongest in GDP/AlF_4^-; intermediate in GTP, GTPγS, and GMPPNP; and lowest in GDP (Fig. 8*A*). Weak dimerization in GDP is consistent with previous gel filtration experiments (13). Indeed, at a lower concentration of cytATL-His, the difference between the GDP and GDP/AlF_4^- samples became more pronounced (Fig. 8*B*). When the concentration of labeled cytATL-His was decreased so that individual particles could be distinguished, the fluorescence of all particles was photobleached in a single step in the presence of GTP, GTPγS, GMPPNP, or GDP, and only a very small fraction was bleached in two steps in GDP/AlF_4^-; the latter is shown in *SI Appendix*, Fig. S10*B* together with data for a control protein. This indicates that most ATL molecules on the membrane were monomeric. The ATL molecules also moved with the expected diffusion constant in the plane of the bilayer (*SI Appendix*, Fig. S10*C*). Presumably, at this low protein concentration, the number of collisional encounters between ATL molecules is insufficient to generate a significant amount of dimers. Taken together, these results show that ATL molecules form cis dimers in a nucleotide-dependent manner.

To determine whether there is competition between cis and trans interactions, we prepared a supported bilayer with Cy3- and Cy5-labeled cytATL-His. After incubation in the presence of different nucleotides, an excess of unlabeled, untagged cytATL was added; a decrease of the FRET signal would indicate that cytATL molecules in bulk solution can associate with labeled cytATL-His molecules on the membrane. Association was observed in the

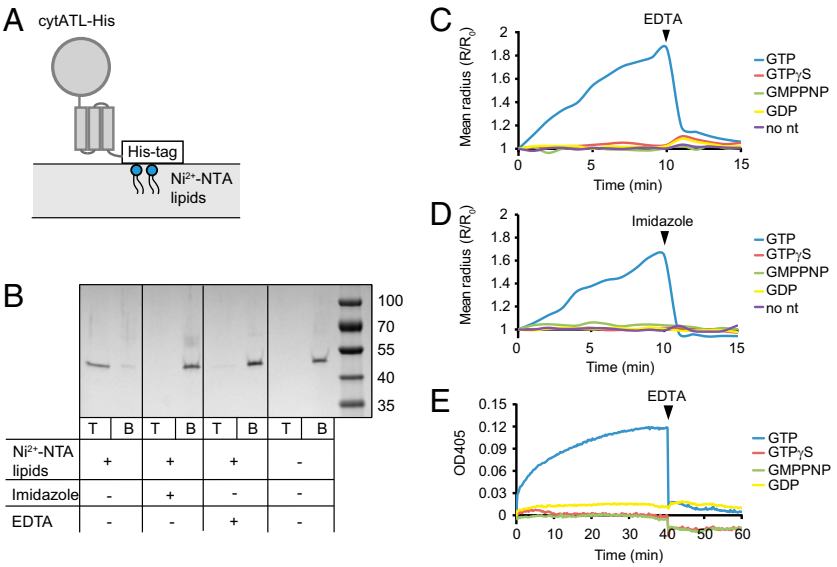

Fig. 5. Membrane tethering mediated by the cytosolic domain of ATL. (*A*) Scheme of cytATL-His in which the TM segments of ATL are replaced by a His_8 tag. The G domain and 3HBs are shown in gray. The protein was bound to vesicles containing Ni^{2+}-NTA–labeled phospholipids. (*B*) Flotation of cytATL-His with Ni^{2+}-NTA–containing vesicles (protein:lipid ratio 1:1,000) in a discontinuous Nycodenz gradient. The top (T) and bottom (B) fractions were analyzed by SDS/PAGE, followed by staining with Coomassie Blue. Where indicated, the vesicles lacked Ni^{2+}-NTA lipids, or the samples were incubated with imidazole or EDTA before flotation. The rightmost lane shows molecular weight markers, with sizes given in kilodaltons. (*C*) The tethering of Ni^{2+}-NTA vesicles containing bound cytATL-His (protein:lipid ratio 1:1,000) was determined by dynamic light scattering in the presence of different nucleotides (no nt, no nucleotide added). EDTA was added after 10 min to inactivate cytATL-His. (*D*) As in *C*, but imidazole was added after 10 min to release cytATL-His from the vesicles. (*E*) As in *C*, but tethering was followed by absorbance at 405 nm, and EDTA was added after 40 min to inactivate cytATL-His.

presence of GTP with high concentrations of added cytATL (Fig. 8*C*). Little or no association of cytATL was observed when the cis dimers were preformed in the presence of GTPγS or GDP/AlF_4^-, respectively (Fig. 8*C*), consistent with decreased dimer dissociation rates in the presence of these nucleotides (Fig. 7*B*). Taken together, these results show that the formation of cis dimers can compete effectively with that of trans dimers, i.e., dimers that result in the fusion of opposing membranes.

A Theoretical Model for Cis and Trans Interactions of ATL Molecules. We developed a theoretical model to test whether competition between cis and trans dimers of ATL can explain the experimental results on vesicle tethering in the presence of different nucleotides. We assumed that two vesicles containing ATL collide by diffusion and allow trans dimer formation when they come closer than the length of the extended ATL dimer (crystal form 2); for steric reasons, only a fraction of the surface area of each vesicle is available for trans dimer formation. Our model considers tethering between vesicles, and not the subsequent step of membrane fusion. Formation of stable tethers was assumed to require simultaneous formation of one or more trans dimers (N = 1, 2...). Competing with trans dimerization, ATL molecules were allowed to form cis dimers in each vesicle with the same rate constants. ATL molecules were initially in a nucleotide-free, monomeric state, and were induced to form cis and trans dimers on the addition of different nucleotides. The calculations used realistic parameters, including the measured on rates and off rates of ATL dimerization in GTP (19) and GDP/AlF_4^- (Fig. 7) (19), the overall rate of GTP hydrolysis as determined by a P_i release assay (19), the radius and concentration of the vesicles, the estimated number of ATL molecules per vesicle used in our experiments, and the length of the cytoplasmic domain of ATL (13, 14) (*SI Appendix*, *SI Materials and Methods*).

In agreement with our experimental observations, the model calculated a low level of tethering in the presence of GDP/AlF_4^-, when dimers form slowly but do not dissociate (Fig. 9, dotted lines); the proportion of tethered vesicles dropped from 15% for N = 1 to 2% for N = 3. When GTP addition was modeled, a much higher level of tethering was calculated (Fig. 9, solid lines). The level decreased with the number of trans dimers required for tethering (increasing N; Fig. 9). The calculations in Fig. 9 assumed that GTP hydrolysis occurs only in dimers, with both ATL molecules hydrolyzing GTP simultaneously, and that the rate constant for P_i release is smaller than that for hydrolysis of the γ-phosphate bond; however, qualitatively similar results were obtained when P_i release was not the rate-limiting step (*SI Appendix*, Fig. S11), or when GTP hydrolysis was allowed to occur in monomers or successively in the two subunits of a dimer. Taken together, our modeling results are in good agreement with the experimental observations, supporting a model in which continuous GTP hydrolysis is required to maintain a pool of ATL monomers on each membrane available for trans dimerization.

Discussion

Our data, together with previous results, lead to the following model of ATL-mediated membrane fusion (Fig. 10). In step 1, ATL monomers bind GTP. This likely requires that the protein be in a conformation corresponding to crystal form 2, because the first helix of the 3HB needs to interact with the base of the G domain for GTP loading (19). Next, the monomers rapidly form a dimer with the bound GTP molecules buried at the interface (steps 2 and 3). This dimer will be weak and transient, and may adopt either a conformation corresponding to crystal form 2 or a conformation in which the G domains are dislodged from the 3HBs and are free to rotate (19). Subsequent GTP hydrolysis converts dimers into the transition state (step 4), in which the dimers adopt a high-affinity state characterized by a tight interaction of the 3HBs. Next, P_i and GDP are released in a consecutive manner (steps 5 and 6), causing the dissociation of the dimer into monomers. Dissociation may occur in the GDP-bound state, in which ATL has a reduced but measurable dimerization propensity (Fig. 8*A*) (13), or it may occur in the nucleotide-free state, in which ATL does not form dimers at all.

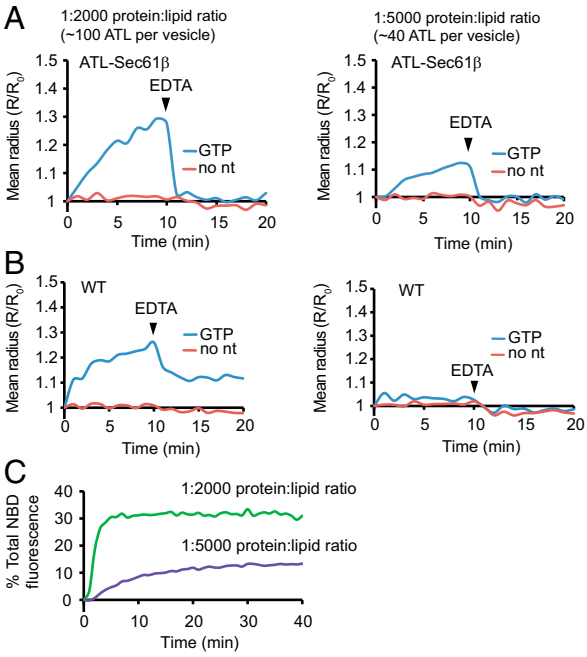

Fig. 6. ATL molecules in a vesicle cooperate to mediate tethering and fusion. (*A*) The tethering of proteoliposomes containing ATL-Sec61β at protein:lipid ratios of 1:2,000 (*Left*) or 1:5,000 (*Right*) was followed by dynamic light scattering in the absence (no nt, no nucleotide) or presence of GTP. The total lipid concentrations in the two reactions were 0.1 mM and 0.25 mM, respectively, and the initial average diameter of the vesicles was ~160 nm, as determined by dynamic light scattering. Thus, the same total number of ATL molecules was distributed over different numbers of vesicles. EDTA was added after 10 min. (*B*) As in *A*, but with WT ATL. (*C*) Membrane fusion of vesicles containing WT ATL at different protein:lipid ratios was followed with a lipid-mixing assay. The lipid concentration was adjusted to keep the total ATL concentration the same in both reactions (0.24 mM for the 1:2,000 reaction and 0.6 mM for the 1:5,000 reaction).

This entire series of events can occur with ATL molecules sitting in the same membranes (cis interactions) or in different membranes (trans interactions), although only trans interactions can result in the tethering and fusion of opposing membranes. Multiple GTPase cycles are required for a successful fusion event, because the transition state dimer formed by ATL molecules sitting in different membranes often completes the cycle of GTP hydrolysis and converts back into monomers before having induced fusion (step 7).

Our results also show that the efficiency of tethering and fusion increases with the density of ATL molecules in the two membranes. With WT ATL molecules, the density at the site of tethering and fusion is further increased by their nucleotide-independent association through their TM segments (24). Fusion may require the cooperation of multiple molecules, because each dimer only forms transiently during GTP hydrolysis; as one dimer dissociates, the presence of other dimers forming nearby would be needed to keep the vesicles tethered. Our results and recent data reported by others (25) also show that tethering of membranes is insufficient to cause membrane fusion; whereas tethering occurs with just the cytoplasmic domains of ATL, fusion requires the native TM segments and is facilitated by an amphipathic helix in the cytosolic C-terminal tail (13, 24).

The crystal structures of ATL are consistent with our proposed model. Crystal form 3 would correspond to the transition state conformation generated both in cis and in trans. The fact that essentially the same conformation was observed with GMPPNP might be explained if GMPPNP did not mimic GTP, but rather induced a state farther along the hydrolysis pathway, or if the conformation was caused by crystal contacts. The dimer observed in crystal form 2 would correspond to a state following GTP loading. The GTP-bound conformation likely adopts several conformations, however, because the 3HBs can undock from the G domain in this state and come closer to one another (Fig. 7) (19). The crystal form 2 dimer also may form in cis, with the 3HBs nearly parallel to the membrane. Crystal form 1 probably forms both in cis and in trans, and likely represents one of the intermediate conformations that the dimer would adopt while converting be-

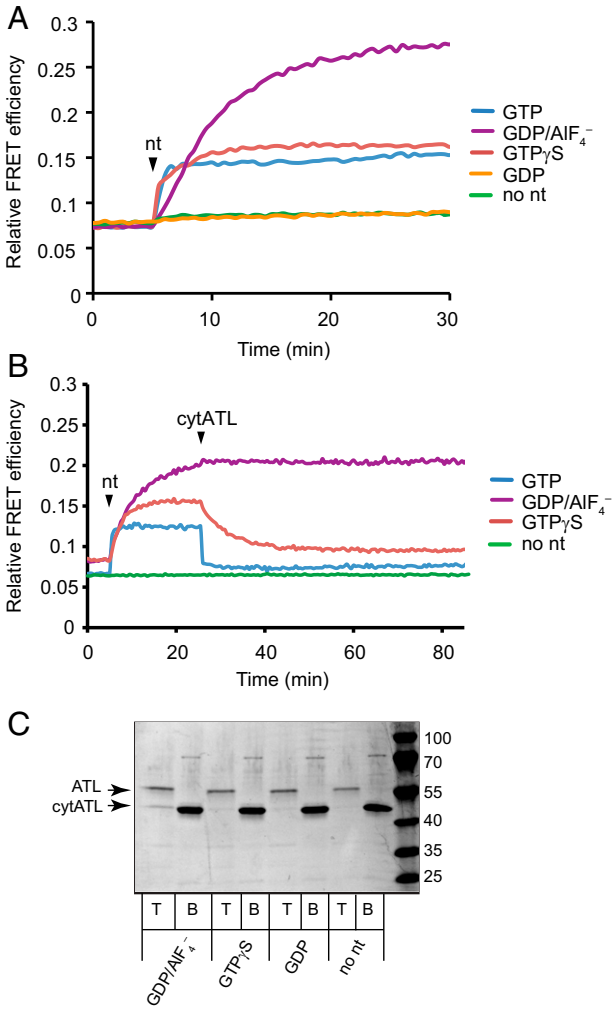

Fig. 7. Nucleotide-dependent dimerization of ATL determined by FRET and coflotation assays. (*A*) The cytosolic domain of *Drosophila* ATL, containing an amber stop codon in the 3HB at position 332, was expressed in *E. coli* in the presence of azidophenylalanine-charged suppressor tRNA. The protein was purified, and the incorporated azidophenylalanine was modified with dibenzocyclooctyne (DBCO)-Cy3 or DBCO-Cy5 fluorescent dyes using Cu^{2+}-free click chemistry. Cy3- and Cy5-labeled proteins were mixed 1:1 (0.5 μM each), and the indicated nucleotide (nt) or no nucleotide (no nt) was added at the indicated time point. FRET was determined by exciting the donor fluorophore (Cy3) at 537 nm and measuring the emission of the donor and acceptor dyes (Cy5) at 570 nm and 667 nm, respectively. FRET is expressed as $I_A/(I_A + I_D)$, where I_A and I_D are fluorescence intensities of the acceptor and donor emission, respectively. (*B*) As in *A*, but 50 μM unlabeled WT cytATL was added to the reactions at the indicated time point. (*C*) Proteoliposomes (1 mM lipids) reconstituted with full-length WT ATL at a protein:lipid ratio of 1:2,000 were mixed with 2 μM cytATL and incubated with GDP/AlF_4^- (1 mM GDP, 0.5 mM $AlCl_3$, and 10 mM NaF), 1 mM GTPγS, 1 mM GDP, or no nucleotide (no nt). The proteoliposome and cytATL mixtures were floated in a discontinuous Nycodenz gradient. The top (T) and bottom (B) fractions of the gradient were analyzed by SDS/PAGE and Coomassie Blue staining. The rightmost lane shows molecular weight markers, with sizes given in kilodaltons.

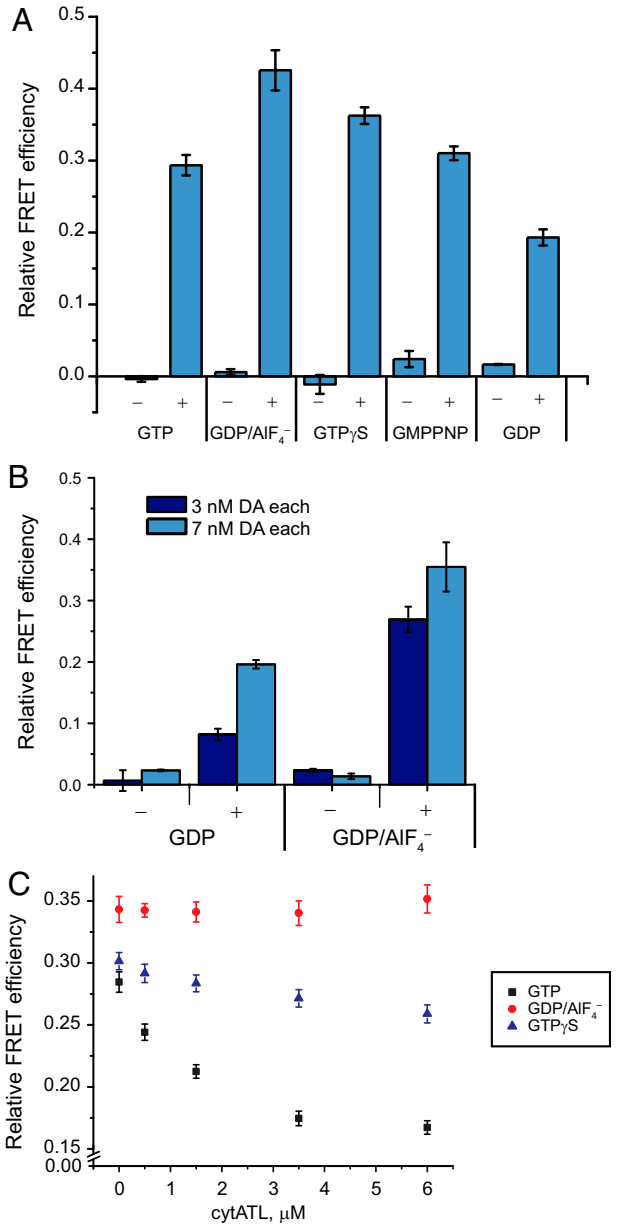

Fig. 8. Nucleotide-dependent cis interactions of ATL on a supported lipid bilayer. (*A*) CytATL-His labeled with Cy3 or Cy5 in the 3HB at position 332 were mixed 1:1 (7 nM each) and added to a supported bilayer containing Ni^{2+}-NTA phospholipids. FRET was determined in a TIRF microscope by exciting the donor dye (Cy3) and measuring the emission of the donor and acceptor (Cy5) dyes. FRET is expressed as $I_A/(I_A + I_D)$, where I_A and I_D are fluorescence intensities of the acceptor and donor emission, corrected for background, bleedthrough of donor emission into the acceptor channel, and direct excitation of the acceptor dye. The indicated nucleotides (1 mM of GTP, GTPγS, or GDP, and GDP/AlF_4^- generated with 1 mM GDP, 0.5 mM $AlCl_3$, and 10 mM NaF) were then added, and FRET was measured again. Shown are the mean and SEM of three independent experiments. (*B*) As in *A*, but with Cy3- and Cy5-labeled cytATL-His mixed 1:1 at 3 nM or 7 nM each. FRET was determined before and after GDP or GDP/AlF_4^- addition. (*C*) As in *A*, except that after incubation of Cy5- and Cy3-labeled cytATL-His on the supported bilayer with the indicated nucleotides, different concentrations of unlabeled WT cytATL lacking a His-tag were added above the supported bilayer. FRET was determined as in *A*.

tween crystal forms 2 and 3. Our model, which takes into account both cis and trans interactions of ATL molecules, removes much of the confusion over how the crystal forms correspond to the stages of membrane fusion.

Our model also explains the puzzling observation that membrane tethering requires GTP hydrolysis, i.e., occurs only with GTP and not with nonhydrolyzable GTP analogs or with GDP/AlF_4^-, despite the fact that the latter conditions cause ATL dimerization (Fig. 7) (13, 14, 19, 22). The difference between GTP and nonhydrolyzable GTP analogs can be explained by the fact that ATL molecules interact most strongly in the transition state of GTP hydrolysis. This enhanced interaction likely involves both the G domains and the 3HBs, as seen in crystal form 3. This is supported by our FRET data, which show that the 3HBs interact more strongly in the transition state than in the GTP-bound state, and by the fact that the G domain alone does not form stable dimers (19, 22). The strong interaction in the transition state would allow ATL molecules in different membranes to tether opposing bilayers. The repulsion of the two membranes in the tethered state and the rigidity of the membranes may be the reason why a tight transition dimer of ATL is required for tethering and why multiple rounds of GTPase cycles are required for fusion. Our results also show that experiments with the cytosolic fragment of ATL in solution can be misleading, because the 3HBs are normally attached to different membranes and thus are restricted in their conformational changes.

Although the foregoing considerations clarify why tethering requires GTP hydrolysis, they do not explain why GDP/AlF_4^- is ineffective, i.e., conditions that mimic the transition state of GTP hydrolysis. Even though ATL molecules associate only slowly under these conditions, some trans dimerization still would be expected after extended time periods. The conundrum is resolved by the observed competition between cis and trans dimers. In the presence of GDP/AlF_4^-, any cis dimers that form would never dissociate (Fig. 7*B* and *SI Appendix*, Fig. S9), leaving no monomers for trans association (Fig. 8*C*). Cis dimerization also may be kinetically favored over trans dimerization. Thus, we propose that a complete GTP hydrolysis cycle is required to generate a pool of monomeric ATL molecules in each membrane, which would then be able to interact in trans, thereby allowing tethering and ultimately fusion of the two opposing membranes. This hypothesis is quantitatively supported by our theoretical model (Fig. 9).

The futile GTPase cycles allowing the assembly and disassembly of cis and trans dimers may seem wasteful; however, such

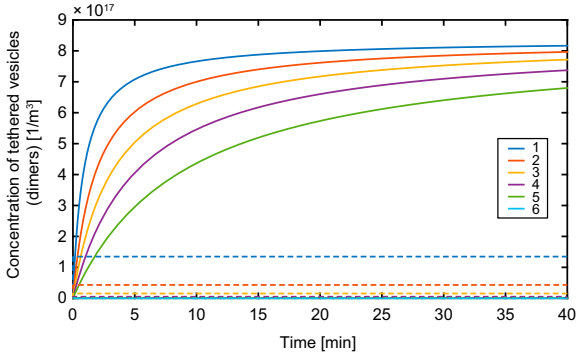

Fig. 9. Theoretical prediction of the time course of ATL-mediated vesicle tethering. Shown is the predicted time course of the generation of paired vesicles, tethered by trans dimers of ATL molecules. The parameters used for the calculations are given in *SI Appendix*. The calculations were performed for conditions in which tethering was initiated by the addition of either GDP/AlF_4^- (broken lines) or GTP (solid lines). Vesicle tethering was modeled with different numbers of trans dimers required for tethering (N = 1–6). GTP hydrolysis was assumed to occur only in dimers, with both ATL molecules hydrolyzing GTP simultaneously. P_i release was assumed to be the rate-limiting step of GTP hydrolysis; the rate constants for P_i release and hydrolysis of the γ-phosphate bond were assumed to be $k_{rel} = 0.08\ s^{-1}$ and $k_{hyd} = 0.76\ s^{-1}$, respectively. Qualitatively similar results were obtained with other scenarios (*SI Appendix*, Fig. S11).

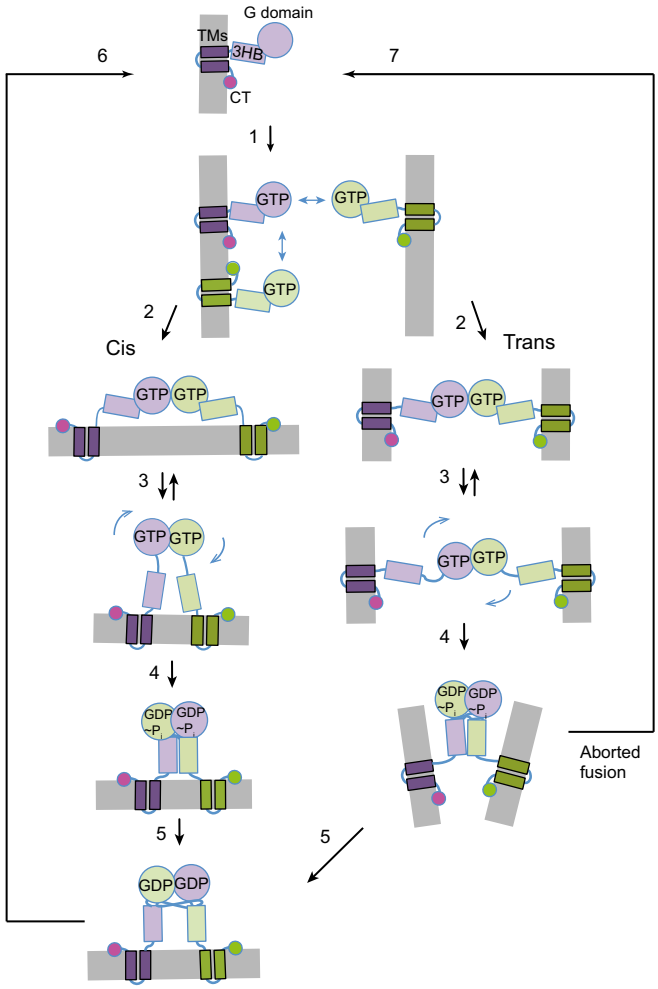

Fig. 10. Model of ATL-mediated fusion. Shown are the different steps of nucleotide-dependent interactions of ATL molecules sitting in the same (cis) or different (trans) membranes. The GTPase (G) domains are shown as circles; the three-helix bundle (3HB) and the two transmembrane segments (TMs), as rectangles; the C-terminal tails (CT), as small circles. The nucleotide state of ATL is indicated. Double-headed blue arrows indicate competition between cis and trans dimer formation. The GTP-bound ATL dimer may equilibrate between two different conformations (indicated by black arrows in the forward and backward direction). Curved blue arrows indicate that the G domain dimer can rotate freely. See the text for details.

cycles also may be viewed as an elegant solution to the problem of mediating multiple rounds of fusion with a single protein. The fusogenic protein molecules have to cycle between being located in the same membranes and in different membranes, and during actual fusion they must interact in a conformation close to either of these situations. In the absence of other factors, at least some cis interactions would be expected, and their disassembly would be required to regenerate monomers. Although it may be assumed that futile cycling is an inherent property of ATL-mediated fusion, a separate biological role is another possibility. For example, it seems possible that cis oligomerization would sequester ATL away from its interaction partners, the reticulons and DP1 (3), which would then allow these curvature-stabilizing proteins to form oligomers on their own. Futile trans dimerization also raises the possibility that an ER network may consist of a mixture of genuine three-way junctions, in which the membranes are fused, and tethered membranes, in which the membranes are not yet fused. The continuous formation and breakage of tethers between membrane tubules might increase the dynamics of ER morphology changes.

Although quantifying the number of futile tethering cycles per fusion event is difficult because of the complex nature of all fusion assays, we obtained a rough estimate from the data in Fig. 1*C* at the lowest GTP concentration (20 μM). Assuming that the added GTP was completely consumed, each ATL molecule hydrolyzed ∼30 molecules of GTP without causing significant fusion in the absorbance assay. This number includes GTP molecules hydrolyzed for futile tethering events as well as for the turnover of cis dimers. This estimate of futile cycling is not necessarily a lower limit, because under these conditions, some low level of fusion was detected with a lipid-mixing assay. It is conceivable that futile GTPase cycles are suppressed in vivo by interactions of ATL with other factors. Although no cytosolic binding partners of ATL have been identified to date, the reticulons, DP1/REEP proteins, and the lunapark protein are all known to associate with the ATLs through their membrane-embedded domains and could potentially regulate ATL's GTPase activity (8, 27, 28).

Our model differs from previously proposed models in several aspects. It was previously suggested that GTP hydrolysis occurs in ATL monomers, which would subsequently form a dimer (19); however, this model implies that the monomers associate with one another when they are in the transition state of GTP hydrolysis, which is unlikely because the monomers associate very slowly in this state (Fig. 7) (19). Rather, the rapid association of monomers in the GTP-bound state suggests that GTP hydrolysis most likely occurs after dimerization. It also has been suggested that tethering does not require the crossover configuration characteristic of crystal forms 1 and 3 and therefore would not involve a strong interaction among the 3HBs (25). This was based on a double mutant of ATL (P319G K320E), which was defective in generating the crossover configuration but was reported to have undiminished GTPase and tethering activity (25). Although we agree that the mutant has GTPase activity similar to that of WT ATL, we found that it is significantly less active in tethering (*SI Appendix*, Fig. S12). In fact, the data of Saini et al. also point in this direction (compare figs 4 and 6F in ref. 25). Thus, it is difficult to make a strong point on the basis of this mutant. Finally, our results exclude the idea that ATL molecules would interact only in cis, rather than tethering opposing membranes before their fusion (23).

It seems possible that aspects of the model for ATL function are relevant to SNARE-mediated membrane fusion, given that SNARE pairing can occur both in cis and in trans. Without involving additional components, a competition between the two pathways seems inevitable, because v- and t-SNARE partners are mixed during multiple fusion events. Although it is possible that certain components, such as tethering factors, prevent cis interactions, it would be important to test for the formation of cis-SNARE complexes with supported bilayers, as done here for ATL. Futile tethering cycles also may be relevant to SNARE-mediated fusion, given that trans-SNARE complexes can be disassembled before they cause fusion (29). Finally, as in the case of ATL, fusion is facilitated when multiple SNARE complexes assemble simultaneously in trans (30).

Materials and Methods

Detailed descriptions of all materials and methods, as well as of the mathematical model, are provided in *SI Appendix, SI Materials and Methods*.

Dynamic Light Scattering. *Drosophila* ATL, ATL-Sec61β, or cyt-TM2 were reconstituted into preformed liposomes as described previously (24). CytATL-His was immobilized on liposomes containing Ni^{2+}-NTA lipids. Proteoliposomes were incubated at 37 °C in a buffer containing 5 mM $MgCl_2$, after which nucleotide (1 mM) was added to start the reaction. After 10 min, EDTA was added to 18 mM to inactivate ATL, or imidazole was added to 150 mM to dissociate cytATL-His from Ni^{2+}-NTA vesicles. Effective hydrodynamic radii

of proteoliposomes were determined with a DynaPro Nanostar instrument (Wyatt). Laser power and attenuation levels were set automatically.

Tethering Assay Using Light Absorbance at 405 nm. GTP, GTPγS, GMPPNP, or GDP was added at 1 mM concentration to proteoliposomes containing WT, mutant ATL, or cytATL-His. For experiments with GDP/AlF_4^-, 1 mM GDP, 10 mM NaF, and 0.5 mM $AlCl_3$, were added sequentially to the reaction. EDTA or imidazole was added after 40 min. Absorbance at 405 nm was measured on a SpectraMax M5 Microplate Reader or Biotek Synergy 4 plate reader. The absorbance before nucleotide addition was set to zero.

Visual Tethering Assay. WT ATL or ATL-Sec61β was reconstituted into preformed liposomes with Texas Red-DPPE or Oregon Green-DPPE (Invitrogen), as described previously (24). The vesicles were mixed 1:1 in a reaction buffer containing 5 mM $MgCl_2$. Different nucleotides were added, and the samples were diluted 1:50 into reaction buffer or buffer with 10 mM EDTA. The samples were spotted onto a glass coverslip and visualized by confocal microscopy. Oregon Green and Texas Red dyes were excited with 491-nm and 561-nm lasers and their emissions selected with 525/50 nm and 620/60 nm filters, respectively. Merged images showing both dyes were generated using Fiji (31).

Flotation Assay. Samples were adjusted to a final concentration of 35% (wt/vol) Nycodenz and overlaid with 25% (wt/vol) Nycodenz and buffer lacking Nycodenz. After centrifugation, fractions were collected from the top of the gradient and analyzed by SDS/PAGE.

Lipid-Mixing Assay. Lipid-mixing assays were performed as described previously (13).

FRET Experiments in Solution. Cy3- and Cy5-labeled cytATL were mixed 1:1 in a reaction buffer containing 5 mM $MgCl_2$, and different nucleotides were added in a 96-well plate. Cy3 was excited at 537 nm, and Cy3 and Cy5 fluorescence emissions were detected at 570 nm and 667 nm, respectively, using a SpectraMax M5 Microplate reader. After 20 min, unlabeled WT cytATL or EDTA was added to the reaction. The relative FRET efficiency was calculated as indicated in the figure legends.

GTPase Assays. The GTPase activities of WT and mutant ATL proteins were determined using the EnzChek phosphate assay kit (Invitrogen), as described previously (13).

Supported Lipid Bilayer Formation. The reaction chamber for supported bilayer experiments was assembled by fixing a plastic ring onto a plasma-cleaned glass coverslip. SUVs (small unilamellar vesicles) were prepared by sonication of an aqueous suspension of lipids [85:15 mol % 1-palmitoyl-2-oleyl-sn-glycerol-3-phosphocholine (POPC):1,2-dioleyl-sn-glycero-3-phosphoserine (DOPS)]. For bilayer formation, the SUVs were incubated in the reaction chamber in the presence of 1 mM $CaCl_2$. Then the reaction chamber was supplemented with 2 mg/mL bovine serum albumin (BSA) for passivation, rinsed thoroughly with buffer, and then resupplemented with 2 mg/mL BSA.

TIRF Microscopy. All reactions were performed in the presence of 5 mM $MgCl_2$ and 2 mg/mL BSA at 23 °C. All images were collected using a Nikon Ti-E motorized inverted microscope equipped with a 100× Plan Apo 1.45-NA TIRF objective lens and a Nikon motorized TIRF illuminator. For FRET experiments, Cy3 and Cy5 dyes were excited with 561-nm and 647-nm lasers, respectively, and their emissions were monitored simultaneously using bandpass emission filters of 510/30 nm and 650/75 nm. For single molecule time-lapse experiments, Cy5 fluorescence was detected with an Andor DU-897 EM-CCD camera, and images were collected at a rate of 20 frames/s with constant illumination and 2 × 2 camera binning.

FRET Measurements and Single-Molecule Tracking on Supported Lipid Bilayers. For FRET experiments, mean fluorescence values were quantified using ImageJ, and relative FRET efficiencies were calculated as described in the figure legends. Single molecules undergoing 2D diffusion on supported bilayers were tracked using tracking algorithms of the U-Track software (32).

ACKNOWLEDGMENTS. We thank the Nikon Imaging Center at Harvard Medical School and Hunter Elliott (Image and Data Analysis Core, Harvard Medical School) for assistance with image collection and analysis; the Institute for Chemistry and Cell Biology screening facility at Harvard Medical School for use of their plate reader; Peter Schultz (Scripps Research Institute) for the pEVOL-AzF vector (26); Dirk Görlich (Max Planck Institute for Biophysical Chemistry) for the K27sumo vector (33); and Benedikt Bauer, Thomas Güttler, and Martin Loose for helpful suggestions on fluorescent labeling of ATL, protein purification, and supported lipid bilayer experiments, respectively. J.H. is supported by the National Natural Science Foundation of China (Grant 31225006), the National Basic Research Program of China (973 Program, Grant 2012CB910302), and an International Early Career Scientist grant from the Howard Hughes Medical Institute. T.Y.L. was supported by a National Science Foundation graduate fellowship. T.A.R. is a Howard Hughes Medical Institute Investigator.

1. Baumann O, Walz B (2001) Endoplasmic reticulum of animal cells and its organization into structural and functional domains. *Int Rev Cytol* 205:149–214.
2. Friedman JR, Voeltz GK (2011) The ER in 3D: A multifunctional dynamic membrane network. *Trends Cell Biol* 21(12):709–717.
3. Hu J, Prinz WA, Rapoport TA (2011) Weaving the web of ER tubules. *Cell* 147(6): 1226–1231.
4. Harrison SC (2008) Viral membrane fusion. *Nat Struct Mol Biol* 15(7):690–698.
5. Wickner W, Schekman R (2008) Membrane fusion. *Nat Struct Mol Biol* 15(7):658–664.
6. Südhof TC, Rothman JE (2009) Membrane fusion: Grappling with SNARE and SM proteins. *Science* 323(5913):474–477.
7. Jahn R, Fasshauer D (2012) Molecular machines governing exocytosis of synaptic vesicles. *Nature* 490(7419):201–207.
8. Hu J, et al. (2009) A class of dynamin-like GTPases involved in the generation of the tubular ER network. *Cell* 138(3):549–561.
9. Orso G, et al. (2009) Homotypic fusion of ER membranes requires the dynamin-like GTPase atlastin. *Nature* 460(7258):978–983.
10. Praefcke GJ, McMahon HT (2004) The dynamin superfamily: Universal membrane tubulation and fission molecules? *Nat Rev Mol Cell Biol* 5(2):133–147.
11. Ferguson SM, De Camilli P (2012) Dynamin, a membrane-remodelling GTPase. *Nat Rev Mol Cell Biol* 13(2):75–88.
12. Rismanchi N, Soderblom C, Stadler J, Zhu PP, Blackstone C (2008) Atlastin GTPases are required for Golgi apparatus and ER morphogenesis. *Hum Mol Genet* 17(11):1591–1604.
13. Bian X, et al. (2011) Structures of the atlastin GTPase provide insight into homotypic fusion of endoplasmic reticulum membranes. *Proc Natl Acad Sci USA* 108(10): 3976–3981.
14. Byrnes LJ, Sondermann H (2011) Structural basis for the nucleotide-dependent dimerization of the large G protein atlastin-1/SPG3A. *Proc Natl Acad Sci USA* 108(6):2216–2221.
15. Wang S, Romano FB, Field CM, Mitchison TJ, Rapoport TA (2013) Multiple mechanisms determine ER network morphology during the cell cycle in *Xenopus* egg extracts. *J Cell Biol* 203(5):801–814.
16. Anwar K, et al. (2012) The dynamin-like GTPase Sey1p mediates homotypic ER fusion in *S. cerevisiae*. *J Cell Biol* 197(2):209–217.
17. Zhang M, et al. (2013) ROOT HAIR DEFECTIVE3 family of dynamin-like GTPases mediates homotypic endoplasmic reticulum fusion and is essential for *Arabidopsis* development. *Plant Physiol* 163(2):713–720.
18. Salinas S, Proukakis C, Crosby A, Warner TT (2008) Hereditary spastic paraplegia: Clinical features and pathogenetic mechanisms. *Lancet Neurol* 7(12):1127–1138.
19. Byrnes LJ, et al. (2013) Structural basis for conformational switching and GTP loading of the large G protein atlastin. *EMBO J* 32(3):369–384.
20. Wu F, Hu X, Bian X, Liu X, Hu J (2015) Comparison of human and *Drosophila* atlastin GTPases. *Protein Cell* 6(2):139–146.
21. Morin-Leisk J, et al. (2011) An intramolecular salt bridge drives the soluble domain of GTP-bound atlastin into the postfusion conformation. *J Cell Biol* 195(4):605–615.
22. Moss TJ, Andreazza C, Verma A, Daga A, McNew JA (2011) Membrane fusion by the GTPase atlastin requires a conserved C-terminal cytoplasmic tail and dimerization through the middle domain. *Proc Natl Acad Sci USA* 108(27):11133–11138.
23. Daumke O, Praefcke GJ (2011) Structural insights into membrane fusion at the endoplasmic reticulum. *Proc Natl Acad Sci USA* 108(6):2175–2176.
24. Liu TY, et al. (2012) Lipid interaction of the C terminus and association of the transmembrane segments facilitate atlastin-mediated homotypic endoplasmic reticulum fusion. *Proc Natl Acad Sci USA* 109(32):E2146–E2154.
25. Saini SG, Liu C, Zhang P, Lee TH (2014) Membrane tethering by the atlastin GTPase depends on GTP hydrolysis but not on forming the cross-over configuration. *Mol Biol Cell* 25(24):3942–3953.
26. Young TS, Ahmad I, Yin JA, Schultz PG (2010) An enhanced system for unnatural amino acid mutagenesis in *E. coli*. *J Mol Biol* 395(2):361–374.
27. Chen S, Novick P, Ferro-Novick S (2012) ER network formation requires a balance of the dynamin-like GTPase Sey1p and the Lunapark family member Lnp1p. *Nat Cell Biol* 14(7):707–716.
28. Park SH, Zhu PP, Parker RL, Blackstone C (2010) Hereditary spastic paraplegia proteins REEP1, spastin, and atlastin-1 coordinate microtubule interactions with the tubular ER network. *J Clin Invest* 120(4):1097–1110.
29. Xu H, Jun Y, Thompson J, Yates J, Wickner W (2010) HOPS prevents the disassembly of trans-SNARE complexes by Sec17p/Sec18p during membrane fusion. *EMBO J* 29(12): 1948–1960.
30. Hernandez JM, Kreutzberger AJ, Kiessling V, Tamm LK, Jahn R (2014) Variable cooperativity in SNARE-mediated membrane fusion. *Proc Natl Acad Sci USA* 111(33): 12037–12042.
31. Schindelin J, et al. (2012) Fiji: An open-source platform for biological-image analysis. *Nat Methods* 9(7):676–682.
32. Jaqaman K, et al. (2008) Robust single-particle tracking in live-cell time-lapse sequences. *Nat Methods* 5(8):695–702.
33. Frey S, Görlich D (2014) A new set of highly efficient, tag-cleaving proteases for purifying recombinant proteins. *J Chromatogr A* 1337:95–105.